

Electronic supplementary information (ESI)

**On the Formation and the Isomer Specific Detection of Methylacetylene
(CH₃CCH), Propene (CH₃CHCH₂), Cyclopropane (c-C₃H₆), Vinylacetylene
(CH₂CHCCH), and 1,3-Butadiene (CH₂CHCHCH₂) from Interstellar
Methane Ice Analogues**

Matthew J. Abplanalp^{1,2}, Sándor Góbi,^{1,2} Ralf I. Kaiser^{*1,2}

**¹ W. M. Keck Research Laboratory in Astrochemistry, University of Hawaii at Manoa,
Honolulu, HI, 96822, USA; ralfk@hawaii.edu**

² Department of Chemistry, University of Hawaii at Manoa, Honolulu, HI, 96822, USA

***Correspondence should be addressed to Ralf I. Kaiser: ralfk@hawaii.edu**

Table of Contents

Calibration ices. A description of the procedure and materials used to determine the vibrational spectra and a PI-ReTOF-MS calibration factor for several of the isomers of interest in this study...S3

Yield calculation. A description of the procedure utilizing the PI-ReTOF-MS calibration factor derived from calibration ices to determine the yield of the isomers of interest in this study...S4

Figure S1. Calibration ice FTIR spectra...S5

Figure S2. FTIR overlay of bands associated with PI-ReTOF-MS TPD profiles of methylacetylene and propene from the irradiated methane ice...S6

Figure S3. PI-ReTOF-MS TPD profiles of methylacetylene, propene, and vinylacetylene at 10.49 eV...S7

Figure S4. Overlay of $m/z = 42$ from irradiated $C_2H_2\text{-}CD_4$ tunable experiments and comparison to $m/z = 42$ from pure irradiated C_2H_2 ...S8

Table S1. Energy dose calculation using CASINO...S9

Table S2. FTIR assignments of pure methylacetylene, propene, vinylacetylene, and 1,3-butadiene at 5 K...S10-S11

Table S3. FTIR assignments of 1% methylacetylene, 1% propene, and 1% 1,3-butadiene in methane at 5 K...S12

Table S4. Photoionization cross sections of the hydrocarbon isomer groups studied...S13

References...S14

Calibration ices. Calibration ices of pure methylacetylene (Organic Technologies, 99%), propene (Aldrich, \geq 99%), 1,3-butadiene (Aldrich, \geq 99%), and 1% methylacetylene, 1% propene, and 1% 1,3-butadiene in methane were also studied (Tables S2 and S3). The pure ices were deposited to thicknesses between 600-700 nm utilizing refractive indices of 1.38, 1.32, 1.39 for methylacetylene, propene, 1,3-butadiene, respectively. The pure ices allowed for the calibration of the infrared absorption coefficients (Table S2) as the amount deposited, measured via laser interferometry, was able to be accurately determined. The experimentally determined absorption coefficients for each of these hydrocarbons was then used to determine the amount of each present in the mixed calibration ice. Next, by monitoring these hydrocarbons via PI-ReTOF-MS the number of integrated counts, corrected for flux and photoionization cross section for each molecule, can be correlated to amount determined to be in the ice. This calibration factor for the PI-ReTOF-MS was then utilized to determine the yield of the C₃ and C₄ products in the irradiated ice.

Yield calculation. Using this PI-ReTOF-MS calibration factor and knowing the dose deposited into the ice via 5 keV electrons from the CASINO calculations (Table S1) allows for the yield per energy deposited of individual molecules to be determined from only PI-ReTOF-MS counts corresponding to a molecule and that molecule's PI cross section (Table S4). For methylacetylene and vinylacetylene no other isomers were detected, and their yields were determined, after flux and photoionization cross section correction, to be $2.17 \pm 0.95 \times 10^{-4}$ and $1.90 \pm 0.84 \times 10^{-5}$ molecules eV⁻¹, respectively (Table 1). However, multiple isomers were detected corresponding to the ion signal of C₃H₆ and C₄H₆. Therefore, to determine the yields of the C₃H₆ isomers the ion signal recorded for m/z = 42 at the photoionization energy of 9.77 eV, which was used to calculate the yield of cyclopropane to be $1.23 \pm 0.77 \times 10^{-4}$ molecules eV⁻¹, was subtracted from its corresponding signal at 10.49 eV. The remaining counts were then used to calculate the yield of propene to be $3.7 \pm 1.5 \times 10^{-3}$ molecules eV⁻¹ (Table 1). Similarly, this was done for the C₄H₆ isomers 1-butyne, 2-butyne, 1,2-butadiene, and 1,3-butadiene utilizing the ion signals from m/z = 54 at photoionization energies of 9.15, 9.45, 9.77, and 10.49 eV, which resulted in yields of $1.28 \pm 0.65 \times 10^{-4}$, $4.01 \pm 1.98 \times 10^{-5}$, $1.97 \pm 0.98 \times 10^{-4}$, and $1.41 \pm 0.72 \times 10^{-4}$ molecules eV⁻¹, respectively.

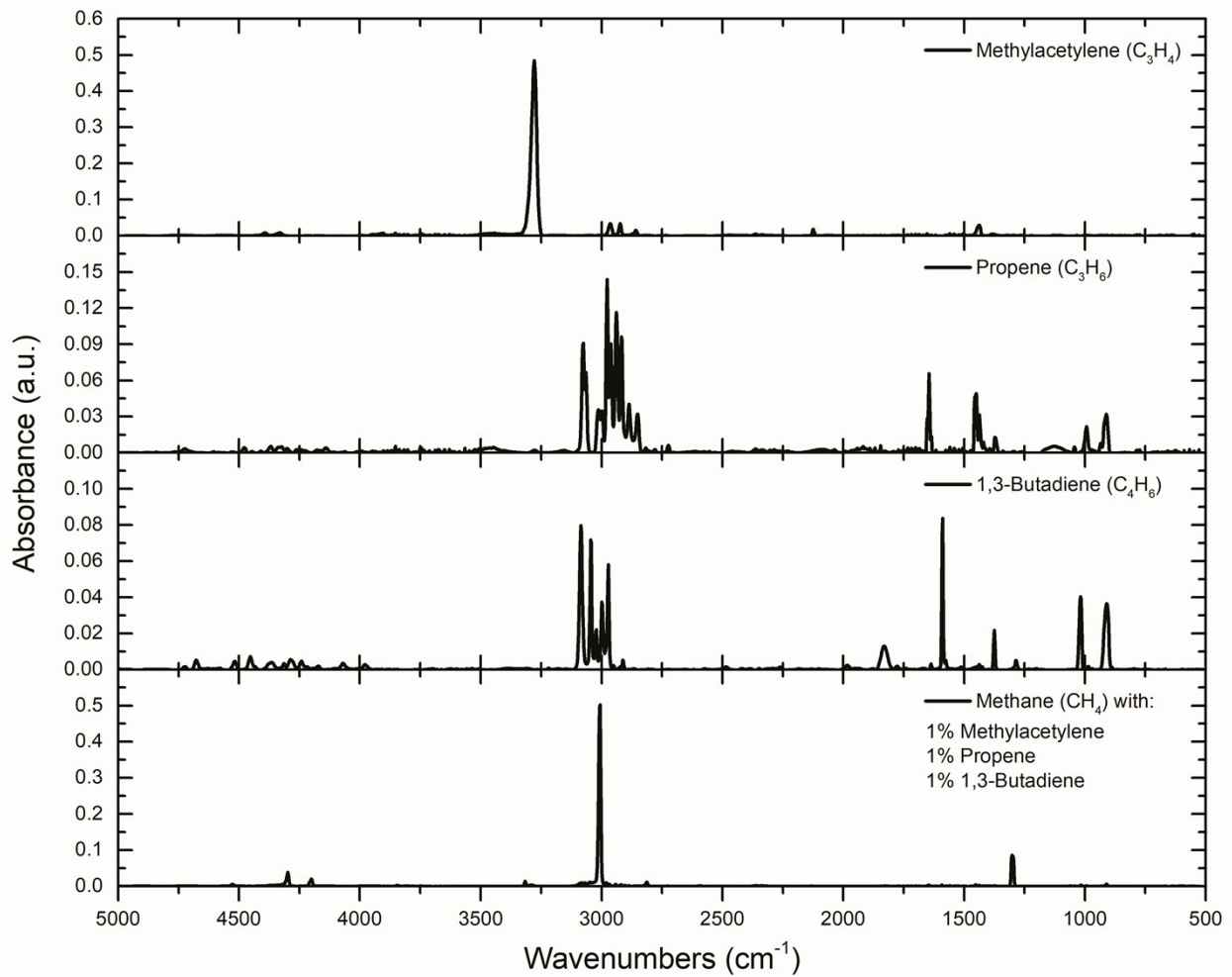


Fig. S1 Infrared spectra from 5000–500 cm^{-1} of calibration ices used for the calibration of the PI-ReTOF-MS signals to determine yields with assignments in Table 2.

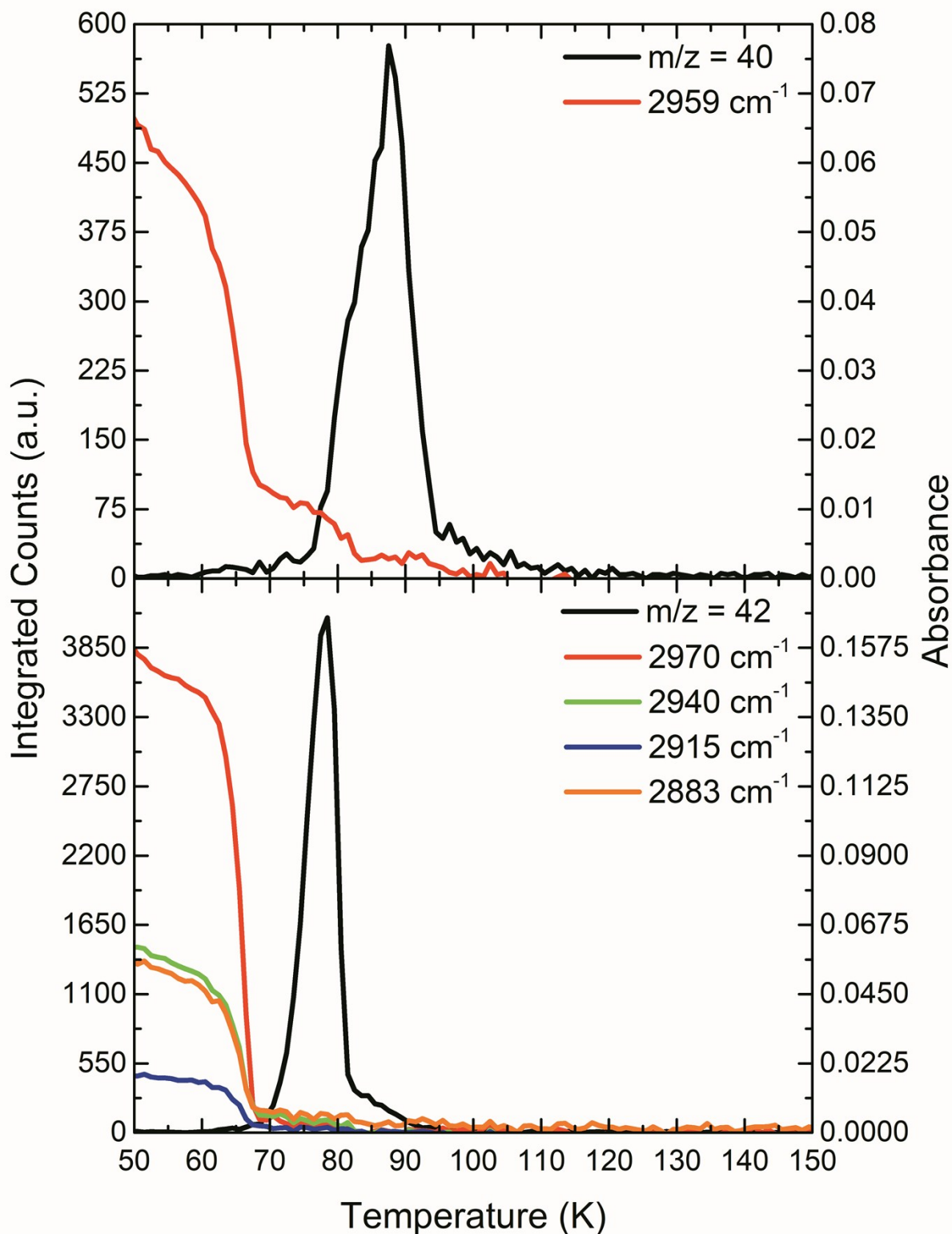


Fig. S2 Overlay of integrated infrared areas corresponding to sublimation events of methylacetylene (top) or propene (bottom) detected from the irradiated methane ice.

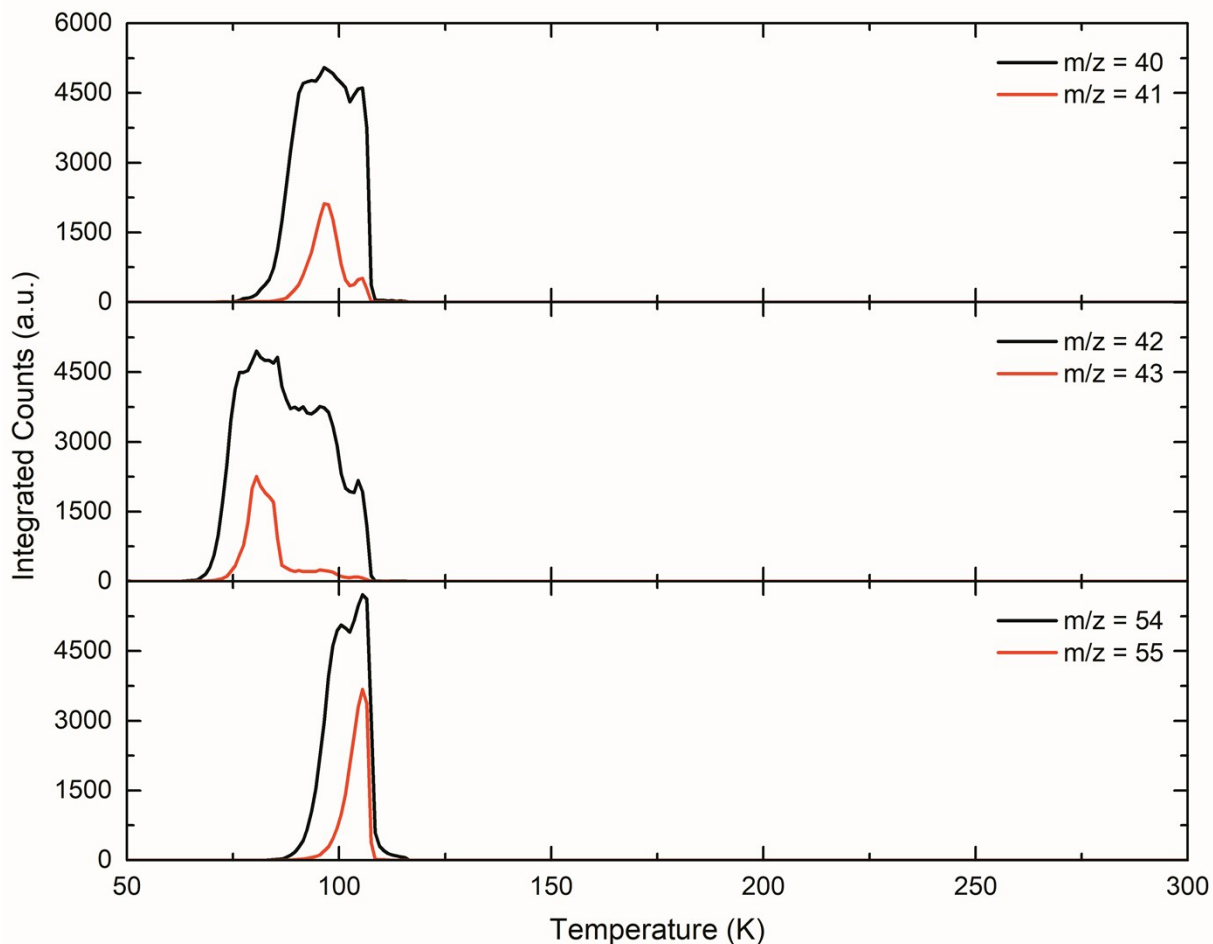


Fig. S3 PI-ReTOF-MS (PI = 10.49 eV) signals recorded during TPD of the calibration ice mixture of methane containing 1% methylacetylene ($m/z = 40$), 1% propene ($m/z = 42$), and 1% 1,3-butadiene ($m/z = 54$) shown in black along with their isotopologues (red).

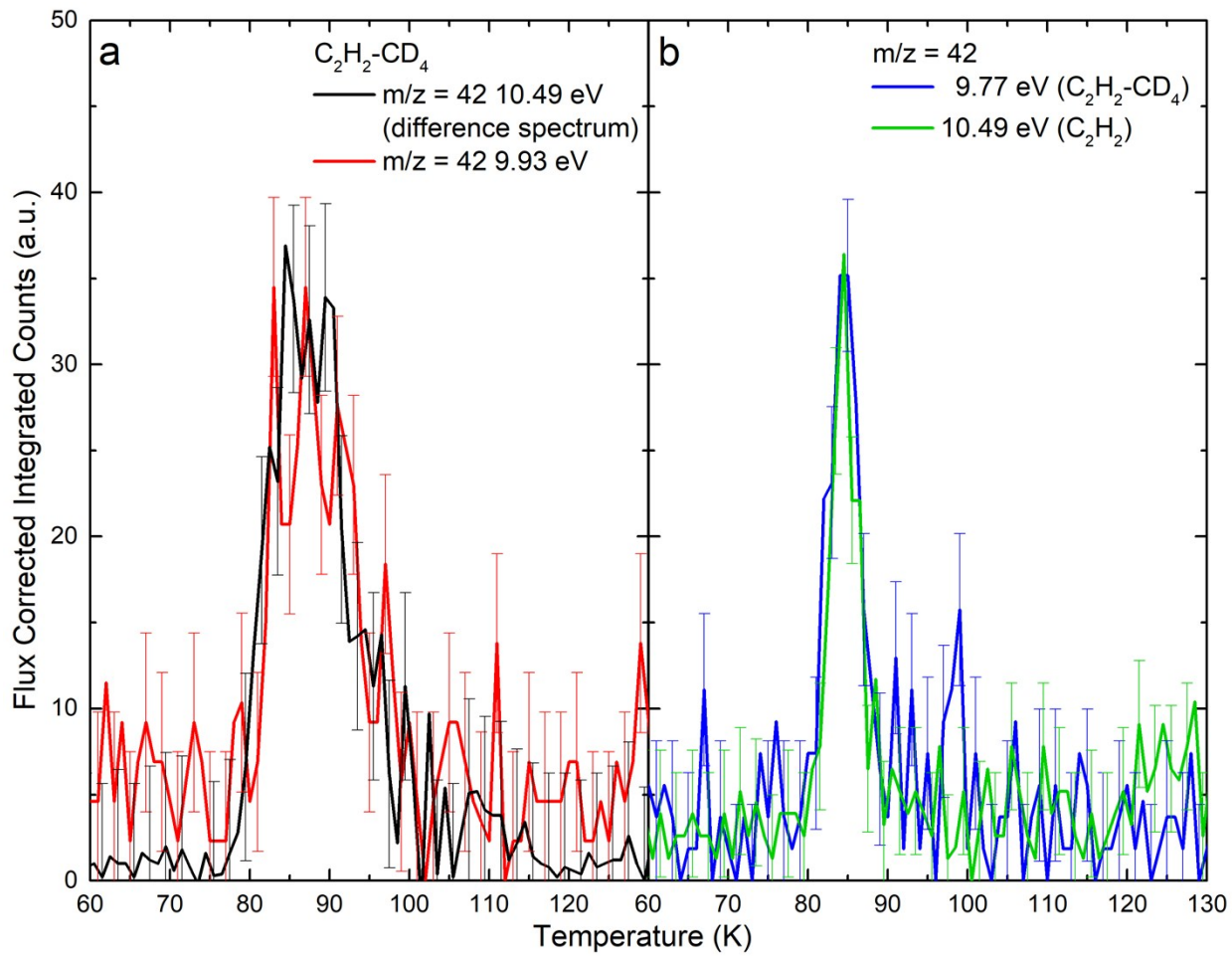


Fig. S4 (a) The residual peak (black) remaining after the subtraction of the scaled methylacetylene peak from the full TPD profile of $m/z = 42$ from the $C_2H_2\text{-CD}_4$ ice, which matches the TPD profile recorded for $m/z = 42$ at PI 9.93 eV (red) which will no longer detect any contribution due to methylacetylene and (b) the profile of $m/z = 42$ recorded using PI = 9.77 eV (blue) which can be due to allene, cyclopropene, and/or propene and $m/z = 42$ recorded using PI = 10.49 eV (green) from irradiated acetylene.

Table S1 Data applied to calculate the average dose per molecule in the methane (CH_4) and mechanism determination ices at 5 K.

	CH ₄ **	C ₂ H ₂ -CD ₄	C ₂ D ₄ -CH ₄	C ₂ D ₂ - ¹³ C ₂ H ₄	C ₂ H ₂
Initial kinetic energy of the electrons, E _{init}	5 keV	5 keV	5 keV	5 keV	5 keV
Irradiation current, I	30 ± 2 nA	20 ± 2 nA	20 ± 2 nA	20 ± 2 nA	20 ± 2 nA
Total number of electrons	(6.7 ± 0.5) × 10 ¹⁴	(1.1 ± 0.1) × 10 ¹⁴	(1.1 ± 0.1) × 10 ¹⁴	(1.1 ± 0.1) × 10 ¹⁴	(1.1 ± 0.1) × 10 ¹⁴
Average kinetic energy of backscattered electrons, E _{bs} *	3.0 ± 0.3 keV	3.2 ± 0.3 keV	3.0 ± 0.3 keV	3.2 ± 0.3 keV	3.2 ± 0.3 keV
Fraction of backscattered electrons, f _{bs} *	0.27 ± 0.03	0.30 ± 0.03	0.28 ± 0.03	0.31 ± 0.03	0.32 ± 0.03
Average kinetic energy of transmitted electrons, E _{trans} *	2.0 ± 0.3 keV	0.1 ± 0.1 keV	0.9 ± 0.3 keV	0.7 ± 0.2 keV	0.9 ± 0.3 keV
Fraction of transmitted electrons, f _{trans} *	0.19 ± 0.01	0.00 ± 0.01	0.01 ± 0.01	0.00 ± 0.01	0.00 ± 0.01
Average penetration depth, l*	410 ± 20 nm	340 ± 20 nm	400 ± 20 nm	320 ± 20 nm	370 ± 20 nm
Density of the ice, ρ	0.47 ± 0.07 g cm ⁻³	0.72 ± 0.09 g cm ⁻³	0.59 ± 0.08 g cm ⁻³	0.82 ± 0.09 g cm ⁻³	0.76 ± 0.09 g cm ⁻³
Irradiated area, A	1.0 ± 0.1 cm ²	1.0 ± 0.1 cm ²	1.0 ± 0.1 cm ²	1.0 ± 0.1 cm ²	1.0 ± 0.1 cm ²
Total molecules processed	(7.3 ± 1.2) × 10 ¹⁷	(6.5 ± 1.2) × 10 ¹⁷	(5.9 ± 0.9) × 10 ¹⁷	(5.5 ± 0.9) × 10 ¹⁷	(6.4 ± 1.2) × 10 ¹⁷
Dose per molecule	3.5 ± 1.1 eV	0.7 ± 0.2 eV	0.8 ± 0.2 eV	0.8 ± 0.2 eV	0.7 ± 0.2 eV

*CASINO values; **Adapted from Abplanalp et al. (2018)

Table S2 Infrared absorption features of pure (a) methylacetylene ice (C_3H_4) (b) propene (C_3H_6) (c) vinylacetylene (C_4H_4) (d) 1,3-butadiene (C_4H_6) at 5 K

Absorptions (cm ⁻¹)	Assignment ^a	Carrier	Integrated Absorption Coefficient	References
(a)				
3280	ν_1	Acetylenic CH stretch	1.22×10^{-17}	a
2964	ν_6	CH ₃ degenerate stretch		a
2923	ν_2	Symmetric methyl CH stretch		a
2858	$\nu_2 + 2\nu_7$	Fermi resonance		a
2123	ν_3	C≡C stretch	1.57×10^{-19}	a
1436	ν_7	CH ₃ degenerate deformation		a
1382	ν_4	CH ₃ symmetric deformation		a
(b)				
3075	ν_1	CH ₂ asymmetric stretch		b,c,d,e
3013	ν_2	CH stretch		b,c,d,e
2978	ν_3	CH ₂ symmetric stretch		b,c,d,e
2941	ν_{15}	CH ₃ asymmetric stretch	1.02×10^{-18}	b,c,d,e
2918	ν_4	CH ₃ symmetric stretch		b,c,d,e
2886	$2\nu_7$	overtone	2.80×10^{-19}	b,c,d,e
2726	$2\nu_9$	overtone	6.17×10^{-20}	b,c,d,e
1645	ν_6	C=C stretch		b,c,d,e
1450	ν_7	CH ₃ asymmetric deformation		b,c,d,e
1437	ν_{16}	CH ₂ scissor		b,c,d,e
1371	ν_9	CH ₃ deformation		b,c,d,e
993	ν_{18}	CH ₂ twist	2.33×10^{-19}	b,c,d,e
911	ν_{19}	C-CH ₃ stretch		b,c,d,e
(c)*				
3912	$\nu_1 + \nu_{11}/\nu_1 + \nu_{17}$	Combination		f,g
3284	ν_1	Acetylenic CH stretch		f,g
3102	ν_2	CH ₂ asymmetric stretch		f,g
3049	ν_3	CH stretch		f,g

3014	ν_4	CH ₂ symmetric stretch	f,g
2973	$\nu_6 + \nu_7$	Combination	f,g
2103	ν_5	C≡C stretch	f,g
1954	$\nu_9 + \nu_{10}$	Combination	f,g
1877	$2\nu_{15}$	Overtone	f,g
1663	$\nu_9 + \nu_{11}$	Combination	f,g
1599	ν_6	C=C stretch	f,g
1418, 1407	ν_7	CH ₂ scissor	f,g
1374	$\nu_{10} + \nu_{12}$	Combination	f,g
128	$\nu_9 + \nu_{12}$	Combination	f,g
1095, 1083	ν_9	CH ₂ rock	f,g
979	ν_{14}	C=C–H bend	f,g
938	ν_{15}	CH ₂ wag	f,g
876	ν_{10}	C–C stretch	f,g
655	ν_{16}	CH ₂ twist	f,g
542	ν_{12}	C=C–C bend	f,g
<hr/>			
(d)			
3086	ν_{17}	CH ₂ asymmetric stretch	h
3044	ν_{18}	CH stretch	h
2972	ν_{19}	CH ₂ symmetric stretch	h
1589	ν_{20}	C=C stretch	h
1374	ν_{21}	CH ₂ scissoring	h
1285	ν_{22}	CH bend	h
1017	ν_{10}	CH bend	h
986	ν_{23}	CH ₂ rock	h
910	ν_{11}	CH ₂ wag	h

References & Notes: ^a (Ball et al. 1994); ^b (Comeford & Gould 1961); ^c(Chao & Zwolinski 1975); ^d(Zaera & Chrysostomou 2000); ^e(Stacchiola et al. 2003); ^f(Kim & Kaiser 2009); ^g(Tørneng et al. 1980); ^h(Hrbek et al. 2007); *adapted from (Kim & Kaiser 2009)

Table S3 Infrared absorption features recorded from calibration mixture methane ices (CH_4) at 5 K containing 1 % methylacetylene (C_3H_4), propene (C_3H_6), and 1,3-butadiene (C_4H_6)

Absorptions (cm^{-1})	Assignment
5989, 5789, 5564, 4528, 4301, 4202, 4114, 3844	$2\nu_3, \nu_1 + \nu_3, \nu_3 + 2\nu_4, \nu_2 + \nu_3, \nu_3 + \nu_4, \nu_1 + \nu_4, \nu_2 + 2\nu_4, 3\nu_4$ (CH_4)
3316	methylacetylene
3290	Methylacetylene
3089	1,3-butadiene
3081	propene
3047	1,3-butadiene
3008	ν_3 (CH_4)
2981	propene
2972	methylacetylene/1,3-butadiene
2941	propene
2919	methylacetylene/propene
2905	ν_1 (CH_4)
2888	propene
2857	methylacetylene
2814	$\nu_2 + \nu_4$ (CH_4)
2726	propene
2591	$2\nu_4$ (CH_4)
2131	methylacetylene
1824	1,3-butadiene
1646	propene
1592	1,3-butadiene
1452	propene
1436	methylacetylene/propene
1377	methylacetylene/1,3-butadiene
1373	propene
1297	ν_4 (CH_4)
1016	1,3-butadiene
993	Propene/1,3-butadiene
910	Propene/1,3-butadiene

Notes: See pure ice Table S2 for details

Table S4 Photoionization cross sections for the C₃H₄, C₃H₆, C₄H₄, and C₄H₆ isomers

Molecule (IE)	Photoionization cross sections (Mb) at specified photoionization energy							References
	10.49 eV	9.93 eV	9.77 eV	9.45 eV	9.15 eV	8.41 eV		
C ₃ H ₄								
Methylacetylene (10.36 eV)	18.9; 23.06; 25.2	-	-	-	-	-	-	a,b,c
Allene (9.69 eV)	15.48; 21.6; 18.9	3.5; 4.4; 3.98	0.64; 0.66; 0.79	-	-	-	-	d,e,f
Cyclopropene (9.67 eV)	8	4	2	-	-	-	-	g
C ₃ H ₆								
Cyclopropane (9.86 eV)	6.57; 6.10	0.05; 0.18	-	-	-	-	-	h,i
Propene (9.73 eV)	9.09; 12; 8.6; 11.092	3.87; -; -; 5.6	1.01; -; -; 2.344	-	-	-	-	a,d,i,j
C ₄ H ₄								
Vinylacetylene (9.58 eV)	32.45	22.08	15.9	-	-	-	-	b
1,2,3,-Butatriene (9.15 eV)	8.17	7.71	6.60	3.35	0.71	-	-	k
Cyclobutadiene (8.16 eV)	12.598	9.74	9.58	7.58	7.42	2.38	-	k
Methylenecyclopropene (8.15 eV)	N/A	N/A	N/A	N/A	N/A	N/A	-	
C ₄ H ₆								
1-Butyne (10.18 eV)	21.82; 20		-	-	-	-	-	a,l
2-Butyne (9.58 eV)	96; 27.7	85.6; 13.18	58.39; 8.96	-	-	-	-	l
1,2-Butadiene (9.23 eV)	14.7	10.45*	9.5	-; (7.2*)	-	-	-	l
1,3-Butadiene (9.07 eV)	16.29; 19; 8.32; 13.2	13.83; -; 7.51; -	13.613; -; 6.995; -	7.62; -; 3.77; -	2.515; -; 1.35; -	-	-	a,b,f,j
C ₄ H ₂								
Diacetylene (10.17 eV)	23.82	-	-	-	-	-	-	b

References & Notes: ^aAdam and Zimmermann (2007); ^bCool et al. (2005); ^cHo and Lin (1998); ^dCool et al. (2003); ^eHolland and Shaw (1999); ^fYang et al. (2012); ^gGoulay et al. (2009); ^hWang et al. (2008); ⁱKoizumi (1991); ^jKanno and Tonokura (2007); ^kestimated; ^lPan et al. (2013); *extrapolated from known values; N/A (not available)

REFERENCES

1. M. J. Abplanalp, B. M. Jones and R. I. Kaiser, *Phys. Chem. Chem. Phys.*, 2018, **20**, 5435-5468.
2. D. W. Ball, R. G. S. Pong and Z. H. Kafafi, *J. Phys. Chem.*, 1994, **98**, 10720-10727.
3. J. Comeford and J. H. Gould, *J. Mol. Spectrosc.*, 1961, **5**, 474-481.
4. J. Chao and B. J. Zwolinski, *Journal of Physical and Chemical Reference Data*, 1975, **4**, 251-262.
5. F. Zaera and D. Chrysostomou, *Surface Science*, 2000, **457**, 71-88.
6. D. Stacchiola, L. Burkholder and W. T. Tysoe, *Surface Science*, 2003, **542**, 129-141.
7. Y. S. Kim and R. I. Kaiser, *Astrophys. J., Suppl. Ser.*, 2009, **181**, 543.
8. E. Tørneng, C. J. Nielsen, P. Klaeboe, H. Hopf and H. Priebe, *Spectrochim. Acta, Part A*, 1980, **36**, 975-987.
9. J. Hrbek, Z. Chang and F. M. Hoffmann, *Surface Science*, 2007, **601**, 1409-1418.
10. T. Adam and R. Zimmermann, *Analytical and bioanalytical chemistry*, 2007, **389**, 1941-1951.
11. T. A. Cool, J. Wang, K. Nakajima, C. A. Taatjes and A. McIlroy, *International Journal of Mass Spectrometry*, 2005, **247**, 18-27.
12. G. H. Ho and M. S. Lin, *J. Chem. Phys.*, 1998, **109**, 5868.
13. T. A. Cool, K. Nakajima, T. A. Mostefaoui, F. Qi, A. McIlroy, P. R. Westmoreland, M. E. Law, L. Poisson, D. S. Peterka and M. Ahmed, *J. Chem. Phys.*, 2003, **119**, 8356-8365.
14. D. M. P. Holland and D. A. Shaw, *Chemical Physics*, 1999, **243**, 333-339.
15. B. Yang, J. Wang, T. A. Cool, N. Hansen, S. Skeen and D. L. Osborn, *International Journal of Mass Spectrometry*, 2012, **309**, 118-128.
16. F. Goulay, A. J. Trevitt, G. Meloni, T. M. Selby, D. L. Osborn, C. A. Taatjes, L. Vereecken and S. R. Leone, *J. Am. Chem. Soc.*, 2009, **131**, 993-1005.
17. J. Wang, B. Yang, T. A. Cool, N. Hansen and T. Kasper, *Int. J. Mass Spec.*, 2008, **269**, 210-220.
18. H. Koizumi, *J. Chem. Phys.*, 1991, **95**, 5846-5852.
19. N. Kanno and K. Tonokura, *Appl. Spectrosc.*, 2007, **61**, 896-902.
20. Y. Pan, Y. Hu, J. Wang, L. Ye, C. Liu and Z. Zhu, *Anal. Chem.*, 2013, **85**, 11993-12001.